Preprints.org

Article

Not peer-reviewed version

# An Experimental Insight on The Use Of N-Butanol as Sustainable Aviation Fuel

Grigore Cican and Radu Mirea *

Posted Date: 10 August 2024

doi: 10.20944/preprints202408.0721.v1

Keywords: butanol; kerosene; aviation; turbo engine; fuel; sustainability

Preprints.org is a free multidiscipline platform providing preprint service that is dedicated to making early versions of research outputs permanently available and citable. Preprints posted at Preprints.org appear in Web of Science, Crossref, Google Scholar, Scilit, Europe PMC.

Copyright: This is an open access article distributed under the Creative Commons Attribution License which permits unrestricted use, distribution, and reproduction in any medium, provided the original work is properly cited.

Preprints.org (www.preprints.org) | NOT PEER-REVIEWED | Posted: 10 August 2024 doi:10.20944/preprints202408.0721.v1

Disclaimer/Publisher's Note: The statements, opinions, and data contained in all publications are solely those of the individual author(s) and contributor(s) and not of MDPI and/or the editor(s). MDPI and/or the editor(s) disclaim responsibility for any injury to people or property resulting from any ideas, methods, instructions, or products referred to in the content.

*Article*

# An Experimental Insight on The Use Of N-Butanol as Sustainable Aviation Fuel

**Grigore Cican [1,2], Radu Mirea[1,*]**

[1] National Research and Development Institute for Gas Turbines COMOTI, 220D Iuliu Maniu, 061126 Bucharest, Romania
[2] Faculty of Aerospace Engineering, National University of Science and Technology Politehnica Bucharest, 1-7 Polizu Street, 1, 011061 Bucharest, Romania
* Correspondence: radu.mirea@comoti.ro

**Abstract:** This study investigates the performance and environmental impact of n-butanol blended with Jet-A fuel in turbo-engines, aiming to assess its viability as a sustainable aviation fuel (SAF). The research involves experimental testing of various blends, ranging from low to high concentrations ofn-buthanol, to determine their effects on engine performance and emissions. The experimental setup includes comprehensive measurements of engine parameters such as thrust, fuel consumption rates, and exhaust gas temperatures. Emissions of sulfur oxide ($SO_2$), and carbon monoxide (COare also analysed to evaluate environmental impacts. Key findings indicate that n-butanol/Jet-A blends can significantly enhance combustion efficiency and reduce emissions compared to conventional Jet-A fuel. Higher n-butanol concentrations lead to improved thermal efficiency and lower $SO_2$ and CO emissions. The study underscores the potential of n-butanol as a SAF for turbo-engines, highlighting its ability to mitigate environmental impacts while maintaining or improving engine performance. This research supports the feasibility of integrating n-butanol into Jet-A blends for turbo-engine applications, emphasizing its role in achieving more environmentally friendly aviation operations.

**Keywords:** butanol; kerosene; aviation; turbo engine; fuel; sustainability

## 1. Introduction

Nowadays research is factored on climate change, biofuels, engine technologies, and the environmental impact of alternative fuels. It highlights the importance of integrating adaptation measures into projections of climate change impacts on health outcomes, noting that doing so generally reduces adverse effects. There is a call for better data and models that account for adaptation dynamically, along with recommendations for policymakers to incorporate these considerations into health planning to mitigate climate change effects more effectively [1].

In the context of biofuels, the current status and future potential within a circular bioeconomy framework is also studied by the various research groups. It discusses various biofuels like biodiesel, bioethanol, and biogas, emphasizing their environmental benefits, such as waste reduction and lower carbon emissions. However, it also points out the economic and policy challenges, underscoring the need for advancements in biotechnological processes and integrated biorefineries to enhance efficiency and sustainability. Also, future directions that include improving feedstock availability, fostering technological innovations, and developing supportive policies to advance a sustainable bioeconomy are suggested and explored [2–5].

There is an underappreciated role of bio-alcohols like methanol, ethanol, and butanol as sustainable aviation fuels, therefore the research indicates that these alcohols improve combustion efficiency and reduce emissions compared to gasoline, with methanol and ethanol being particularly effective. The studies highlight the environmental and performance benefits of using these alcohols in turbocharged spark-ignition engines and as additives to gasoline. However, the text also notes that while ethanol and methanol blends enhance engine efficiency and reduce emissions, butanol slightly increases CO emissions. Overall, hydrogen emerges as the most sustainable option for reducing greenhouse gas emissions, especially when produced from renewable sources [6–9].

© 2024 by the author(s). Distributed under a Creative Commons CC BY license.

Preprints.org (www.preprints.org) | NOT PEER-REVIEWED | Posted: 10 August 2024 doi:10.20944/preprints202408.0721.v1



Finally, the influence of bio-alcohols on engine performance is studied, particularly in ethanol-gasoline blends. Studies show that these blends improve combustion efficiency and reduce emissions, although they may increase fuel consumption due to ethanol's lower energy density. Of great importance are government policies in ethanol production, particularly in the U.S., where policies like the Renewable Fuel Standard (RFS) have played a critical role. It emphasizes the environmental benefits of ethanol and other alcohol fuels but stresses the need to balance policy, market conditions, and technological advancements for future growth [10–12].

As for the usage of alcohols in turbo-engines, multiple studies on alternative fuels for aviation engines were undertaken. They evaluate biodiesel-based sustainable aviation fuel (SAF) in turbo-engines, finding that it reduces CO2 and NOx emissions while maintaining stable performance akin to conventional jet fuel [13]. Also, they explore recycled sunflower and palm oil-derived biodiesel in microturbo-engines, highlighting its environmental benefits and improved engine performance[14], they examine various alternative fuels in microturbine and turbofan engines, showing they can sustain or enhance performance while reducing NOx and particulate emissions [15] and, they investigate ethanol blends with Jet A-1 fuel, demonstrating improved combustion efficiency and reduced emissions, indicating ethanol's potential to enhance aviation sustainability. Collectively, these studies underscore the promise of biodiesel and ethanol blends in advancing aviation's environmental sustainability through reduced emissions and improved engine performance [16].

There are also papers that examines the certification process of adapting a carburetor aircraft engine to run on ethanol fuel, discussing technical and regulatory considerations. It emphasizes the observed performance and emission characteristics during testing, demonstrating ethanol's feasibility as an alternative fuel for light aircraft and highlighting its environmental benefits. Litt et al. simulate the effects of alternative fuels in turbofan engines, employing advanced modeling to evaluate their impact on performance and emissions. Their study provides insights into how these fuels can potentially mitigate environmental impacts in commercial aviation. Additionally, Gawron et al. investigate a miniature turbojet engine fueled by Jet A-1 blended with alcohol, analyzing combustion efficiency and emissions such as NOx and particulate matter. Their findings suggest alcohol blends can improve combustion efficiency and reduce emissions, particularly beneficial for small-scale turbojet applications. Collectively, these studies underscore the advantages of ethanol in light aircraft, the simulation benefits for turbofan engines, and performance enhancements with alcohol blends in miniature turbojets, contributing to sustainable aviation by enhancing engine efficiency and reducing emissions [17–20].

Blends of alcohols and different aviation fuels have been studied in terms of engines' performances, gaseous emissions and overall their usage as SAF like ethanol's application in small turbojet engines, emphasizing its potential to improve engine performance and reduce emissions, thereby promoting its role as a sustainable aviation fuel [21]. Cican et al. [22] analyze bioethanol blends in micro turbo-jet engines, finding they enhance combustion efficiency and lower emissions, highlighting their suitability for micro-turbojet applications. Some researchers experiment with butyl butyrate and ethanol blends in gas turbine combustors, demonstrating their ability to reduce emissions and enhance combustion efficiency [23]. Additionally, Cican et al. evaluate methanol/Jet-A blends for turbo-engines, showing promising results in improving engine efficiency and reducing environmental impact. Together, these studies underscore advancements in alternative fuels such as ethanol, bioethanol blends, butyl butyrate, and methanol, showing their potential to enhance both performance and sustainability in aviation. Ongoing research promises further improvements in efficiency and environmental benefits, contributing to the evolution of more sustainable aviation propulsion systems [24].

The paper explores the use of n-butanol in a compact turbojet engine, aiming to assess its feasibility in a Jet A/n-butanol blend as a potential fuel for small turbojet engines. Building on prior research, the study focuses on evaluating operational parameters of micro turbo-engines used in drones and aero-models. Additionally, it investigates transient processes, including engine stability during start-up, abrupt accelerations, and decelerations, while analysing emissions like CO and SO2.

Preprints.org (www.preprints.org) | NOT PEER-REVIEWED | Posted: 10 August 2024 doi:10.20944/preprints202408.0721.v1



The research involves varying Jet A/n-butanol blend compositions, comparing them against a benchmark blend of Jet A with 5% Aeroshell 500 Oil (Ke). Specifically, blends with 10%, 20%, and 30% n-butanol are analysed to understand their impact on engine performance and emissions. This comparative analysis aims to provide insights and take a step forward into the potential benefits and challenges of using n-butanol as a renewable component in aviation fuel blends, potentially advancing the development of more sustainable and efficient micro turbojet engines for unmanned aerial vehicles (UAVs) and similar applications.

## 2. Materials and Methods

Four types of fuels were examined: Jet A aviationfuel + 5% Aeroshell 500 Oil (Ke), n-butanol(B) and blends of Ke+10%B, Ke+20%B, and Ke+30%B, these are mass percentages. This chapter will detail the experimental evaluation of several physical-chemical properties of the fuel samples. Additionally, testing will be performed by running a micro turbo-jetengine on these fuels and blends.

### *2.1. Blends characterization*

The fuel characterization was carried out experimentally by measuring various parameters such as density, kinematic viscosity, flash point, lower calorific value, FT-IR analysis and elemental analysis.

Density was measured for all samples at a temperature of 22 degrees Celsius following SR EN ISO 3675/2002 standards[25], using a graduated cylinder and a thermal densimeter manufactured by Termodensirom SA, Bucharest, Romania. Flash point was determined for all samples according to ASTM D92 standards[26], using an Cleveland flash point tester provided by Scavini, Italy. Kinematic viscosity was measured for all samples at 40 degrees Celsius in accordance with SR EN ISO 3104/2002 standards[27], using a viscometer supplied by Scavini, Italy. The lower calorific value was determined for all samples following ASTM D240-17 standards[28], There was used an IKA WERKE C 2000 calorimeter sourced from Cole-Parmer, St. Neots, United Kingdom, and a C 5012 calorimeter bomb manufactured by IKA Analisentechnik GmbH, Staufen, Germany. Fourier Transform Infrared Spectroscopy (FTIR) analysis was conducted using a Spectrum Oil Express Series 100 spectrometer, version 3.0, provided by Perkin Elmer, Romanian representative located in Tâncăbești, Romania, along with its dedicated software.

Elemental analysis was performed on all five samples to identify the primary elements (C, N, H, O), following the ASTM D 5291-16 standards[29].

Further details about the fuel characterization process can be found in [24].

### *2.2. Theoretical combustion process*

After determining the elemental composition, the minimum air quantities required for stoichiometric combustion for Jet A + 5% Aeroshell 500, butanol (B), and the respective blends were calculated, as well as the resulting amounts of $CO_2$ and $H_2O$ from stoichiometric combustion.

For the necessary calculations, the general formula considered for hydrocarbons is of the form CcHhOo [24], with specific fractions for each element gC, gH, gO, and gN. Calculating the required amount of oxygen for stoichiometric combustion is essential for obtaining information about the combustion process and facilitating a comprehensive understanding of the involved chemical reactions. This can be achieved using equation 1.

$$M_o = 2.667gC + 8gH - gO \quad (1)$$

Using formula 1 the quantity of air for stoichiometric combustion can be calculated.

$$M_{air} = 4.35M_o \quad (2)$$

Using formulas 3 and 4, the quantity of $CO_2$ and $H_2O$ produced during the combustion process can be calculated.

$$CO_2 = 44\frac{gC}{12} \quad (3)$$

Preprints.org (www.preprints.org) | NOT PEER-REVIEWED | Posted: 10 August 2024 doi:10.20944/preprints202408.0721.v1



$$H_2O = 9gH \quad (4)$$

*2.3. Turbo Engine Testing Methodology*

The experiments were conducted using the Jet CAT P80® micro turbojet-engine [30]. Figure 1 shows the test stand and its main components.

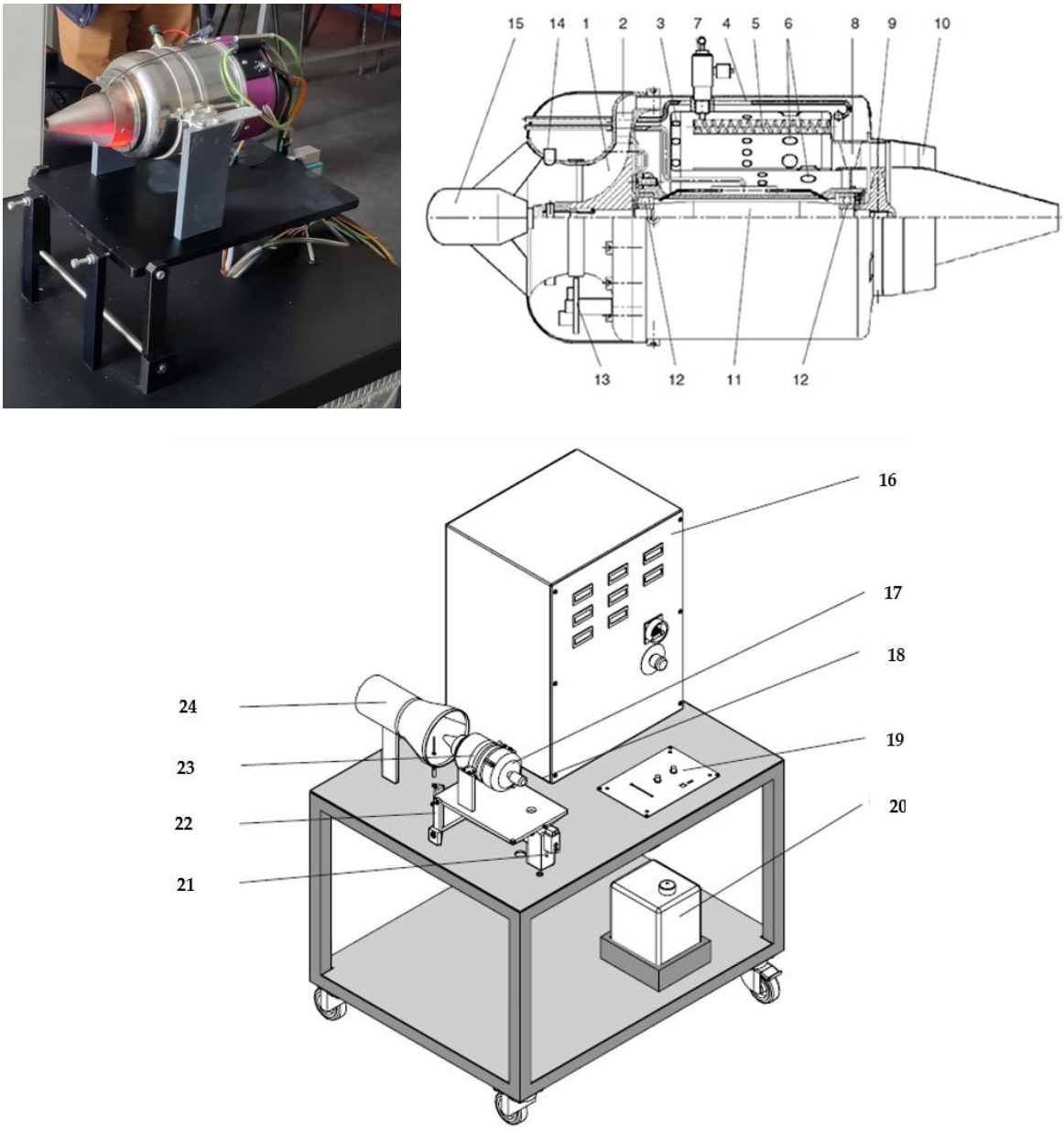


**Figure 1.** The microturbine engine test stand.

The turbo-engine consists of an axial turbine linked directly to a radial compressor and an annular combustion chamber. These elements, along with the intermediate bearing housing, form a compact unit originally intended for use in model airplanes. The process starts with the rapid rotation of the compressor wheel (1), which spins at speeds between 35,000 and 115,000 rpm, accelerating the intake air. This air then enters the aluminum diffuser (2), where its kinetic energy is converted into pressure.

At the inlet of the combustion chamber (3), a portion of the air is redirected to the front of the flame tube (4). Simultaneously, liquid fuel is introduced from the rear into specialized evaporator tubes (5) where it is converted into gas. This gaseous fuel is then mixed with the primary air towards the front of the combustion chamber and ignited. The flame tube is cooled externally by secondary

Preprints.org (www.preprints.org) | NOT PEER-REVIEWED | Posted: 10 August 2024 doi:10.20944/preprints202408.0721.v1



air, channeled through bores (6), to reduce the extremely high combustion temperatures (approximately 2000°C) to the acceptable turbine inlet temperature range of 600–800°C. An igniter glow plug (7) initiates the combustion process during startup. The resulting combustion gases flow into the turbine's diffuser (8), gaining velocity before entering the axial wheel (9). In the turbine, these gases transfer their energy to drive the compressor wheel, experiencing partial relaxation and cooling in the process. Finally, the gases are expelled through the thrust nozzle (10) at approximately 600°C. The turbine and compressor wheels are mounted on a shared shaft (11), which is supported by ball bearings (12) within the bearing housing and cooled by the compressor air. The front hood contains the electronics (13) responsible for the starter motor (15), temperature monitoring, and speed measurement (14).

Additional components include: (16) the switch cupboard with indicators; (17) the inlet nozzle for air flow measurement; (18) the turbine desk; (19) the gas turbine control panel; (20) the fuel tank; (21) the force sensor for thrust measurement; (22) the bearing of the turbine desk; (23) the jet turbine; and (24) the mixing tube.

The micro turbojet engine used for the experiments is of the turbojet type, as shown in Figure 1. More information about its description can be found in [34]. To record the parameters of interest during the experiments, a series of sensors measure and record thrust, temperature in front of the turbine, temperature after the compressor, RPM, pressure at the combustion chamber outlet, fuel flow, and airflow. The instrumentation of the micro turbojet engine allows continuous recording of all these parameters at intervals of one second.

Since this type of turbojet engine is not equipped with an oil pump, the bearings are lubricated with fuel, and therefore 5% Aeroshell 500 oil is added to the fuel. Tests were conducted under the three most important operating regimes of the micro turbojet engine: idle, cruise, and maximum. To ensure better measurement accuracy, the micro turbojet engine was maintained in each regime for approximately two minutes, during which time the parameters were recorded and averaged.

The operating principle of the micro turbojet engine is constant RPM, so for each regime studied, the engine maintained the same RPM regardless of the fuel type. To adhere to this operating principle, the fuel flow was adjusted so that, regardless of the fuel type, the engine maintained a constant RPM.

### *2.4. Gaseous emissions measurements*

The gaseous emission measurements were conducted using the MRU Vario Plus analyzer (Messgeräte für Rauchgase und Umweltschutz GmbH, Neckarsulm-Obereisesheim, Germany), as shown in Fig. 2. Simultaneously, the analyzer measured various gas components, including $O_2$, CO, NO, $NO_2$, NOx, $SO_2$, and $CH_4$.

Since this study monitored the concentration of $SO_2$ and CO, the measuring range and accuracy of the measurements for these gases are presented below.

The measuring range for sulfur dioxide ($SO_2$) was 0–2000 ppm with an accuracy of ±10 ppm or 5% of the reading for concentrations below 2000 ppm, and 10% of the reading for concentrations above 2000 ppm. For carbon monoxide (CO), the measuring range was 0–4000 ppm with an accuracy of ±10 ppm or 5% of the reading for concentrations below 4000 ppm, and 10% of the reading for concentrations above 4000 ppm.

**Figure 2.** MRU Analyzer.

Preprints.org (www.preprints.org) | NOT PEER-REVIEWED | Posted: 10 August 2024 doi:10.20944/preprints202408.0721.v1



## 3. Results and discussion

### *3.1. Experimental results for the physical-chemical properties of fuel blends*

The experimentally determined values for the physico-chemical properties are presented in Table 1

**Table 1.** The experimentally determined values for the physico-chemical properties.

| Sample | Flash Point [°C] | Kinematic viscosity at 40 °C [cSt] | Density at 22 °C [g/cm³] | Low Calorific Power [kJ/kg] | Elemental analysis |
|---|---|---|---|---|---|
| **Ke** | 42.3 | 1.39 | 0.817 | 42.39 | C% = 85.17<br>H% = 13.31<br>N% = 0.07<br>O% = 1.45 |
| **Ke + 10%B** | 33.9 | 1,51 | 0,816 | 40.93 | C%=83,13<br>H% =13.33<br>N% =0.06<br>O% =3.46 |
| **Ke + 20%B** | 33.7 | 1,63 | 0,816 | 39.46 | C%=81,09<br>H% =13.35<br>N% =0.06<br>O% =5.48 |
| **Ke + 30%B** | 33.1 | 1,74 | 0,815 | 37,99 | C%=79,05<br>H% =13.36<br>N% =0.05<br>O% =7.49 |
| **B** | 35 | 2.573 | 0.81 | 27.7 | C%=64,76<br>H% =13.49<br>N% =0<br>O% =21.59 |

Based on the data from Table 1, Elemental analysis shows that the carbon and hydrogen content decreases as the alcohol concentration in blends increases, while the oxygen content increases. This change can reduce CO2 emissions during combustion due to reduced oxygen demand. Additionally, the flash point, kinematic viscosity, and density decrease proportionally with the increase in alcohol percentage, highlighting its significant impact on physical properties. FT-IR analysis is essential for detecting chemical changes in fuels, especially when alcohols or biodiesel are added. The FTIR spectra presented in Figure 3 reflect the changes in Ke, Ke+10%B, Ke+20%B, Ke+30%B, and 100% B.

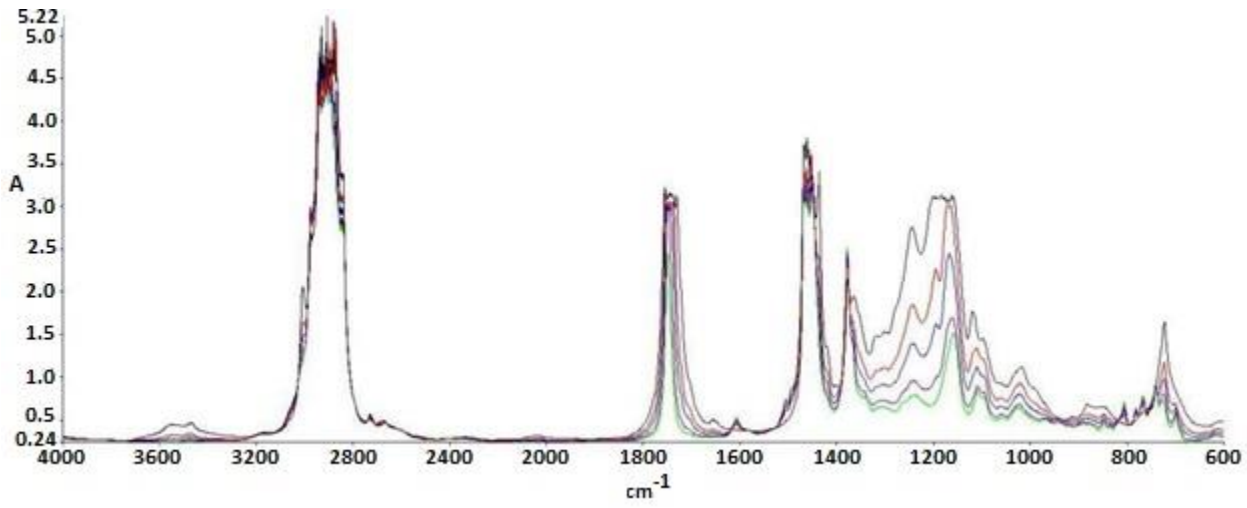

Preprints.org (www.preprints.org) | NOT PEER-REVIEWED | Posted: 10 August 2024 doi:10.20944/preprints202408.0721.v1



**Figure 3.** FTIR spectra of Ke (green), Ke + 10%B (purple), Ke + 20%B (clue), Ke + 30%B (red) and 100% B (black).

- The main differences between the spectra of conventional aviation fuel (Ke) and the blends are observed at 3200-3600 cm-1 in Figure 3, indicating the introduction of the hydroxyl group (-O-H) into the molecular structure.
- Higher alcohol concentrations result in larger peaks in the mentioned spectra.
- At 1750 cm-1, the presence of oxygen bonded to a carbon atom (C-O) is highlighted.
- Methylene groups (-CH2) at 1450 cm-1 show a slight decrease compared to the Ke spectrum.
- Radiation absorbed at 1350 cm-1 shows an increase in methyl groups (–CH3).
- At 1000 cm-1, the C-OH bond is highlighted, which increases with alcohol concentration, similar to the –OH group.
- The intensities of these features were observed to increase with alcohol concentration in each of the analyzed spectra. [32]

*3.2. Combustion reaction analysis*

According to equations 1-4, the summarized values are displayed in Table 2, where Mo denotes the oxygen quantity needed for the stoichiometric reaction, Mair indicates the required air quantity, and $CO_2$ and $H_2O$ represent the quantities of carbon dioxide and water produced from the combustion of one kilogram of fuel at stoichiometric conditions.

**Table 2.** Calculated values for 1 kilogram of fuel blend.

| Blend | MO [kg] | Mair [kg] | CO2 [kg] | H2O [kg] |
|---|---|---|---|---|
| **Ke+5% Aeroshell 500 Oil** | 3.32 | 14.45 | 3.12 | 1.20 |
| **Ke+10%B** | 3.25 | 14.13 | 3.05 | 1.20 |
| **Ke+20%B** | 3.18 | 13.82 | 2.97 | 1.20 |
| **Ke+30%B** | 3.10 | 13.49 | 2.90 | 1.20 |
| **B** | 2.67 | 11.60 | 2.37 | 1.21 |

A reverse correlation is observed between the necessary air volume and the concentration of alcohol. This trend is linked to a rise in oxygen levels as alcohol concentrations increase. Moreover, there's a consistent decrease in $CO_2$ levels with higher alcohol concentrations. These observations emphasize the complex interaction among alcohol content, oxygen levels, and resulting $CO_2$ concentrations during the stoichiometric combustion process.

*3.3. Microturbojet engine test stand experiments*

The starting procedure of turbo engines is a process that concludes when the turbo engine reaches idle mode. The primary aim of this test is to evaluate the ignition process when the micro-turbo-engine operates with the four studied fuel types. Figure 4 depict the variation of the micro-turbine engine speed over time, while Figures 5 and 6 illustrate the variation of combustion temperature and fuel flow rate as a function of engine speed.

Preprints.org (www.preprints.org) | NOT PEER-REVIEWED | Posted: 10 August 2024 doi:10.20944/preprints202408.0721.v1



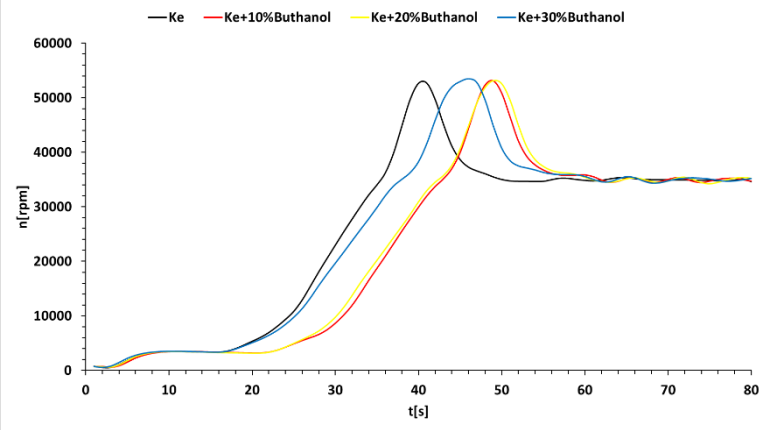


**Figure 4.** The variation of n with respect to time.

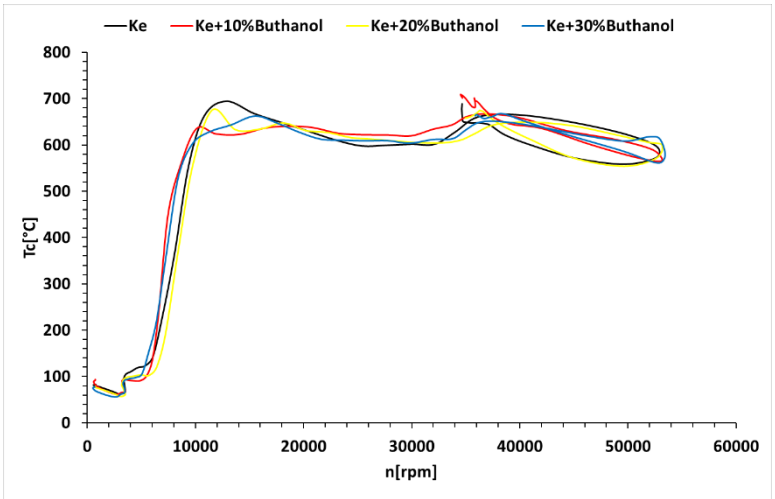


**Figure 5.** The variation of T_comb with respect to RPM.

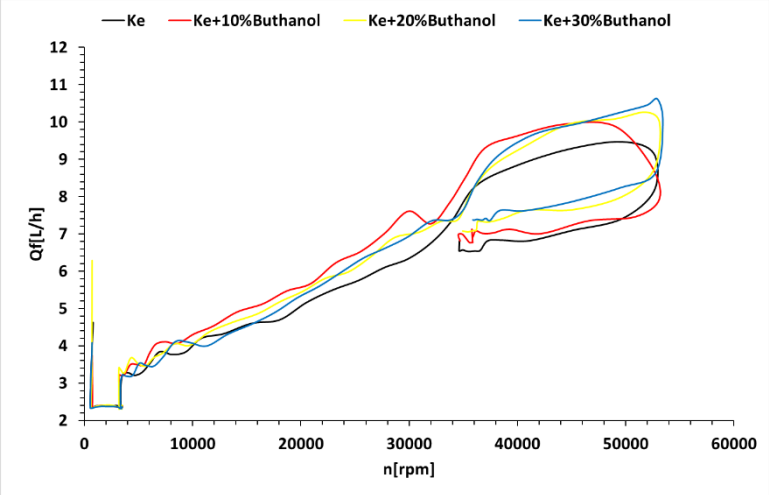


**Figure 6.** The variation of fuel flow with respect to RPM.

Figure 4 demonstrates a correlation between starting time and the concentration of n-butanol, with Ke showing the shortest starting time. Figure 5 indicates a minor decrease in fuel temperature during the starting process, attributed to the influx of outside air into the combustion chamber by the electric starter. Moreover, the ignition timeframe, as depicted in Figure 5, extends with higher n-butanol concentrations. Additionally, Figure 5 shows that as the alcohol concentration increases, the temperature ahead of the turbine decreases during the starting process, resulting in a delay. Figure 6

Preprints.org (www.preprints.org) | NOT PEER-REVIEWED | Posted: 10 August 2024 doi:10.20944/preprints202408.0721.v1



highlights a reduction in the fuel flow rate required for the starting process with increasing n-butanol concentration. This is attributed to Ke's higher starting temperature, which necessitates a larger initial fuel quantity. However, after reaching the operating temperature, the variation in fuel flow rate reverses, indicating higher rates for fuel blends and lower rates for Ke. This dynamic interaction is essential for comprehending the behavior of fuel blends during both the initial "cold" phase and subsequent operational periods of the starting procedure.

To evaluate the microturbojet engine's stability regarding the combustion process, a sudden procedure was performed.

This involved rapidly accelerating from idle to maximum, maintaining maximum speed for 30 seconds, and then decelerating abruptly from maximum to idle. Figures 7–9 depict variations in temperature ahead of the turbine, fuel flow rate, and thrust as a function of RPM during rapid acceleration and deceleration for all four fuel samples studied.

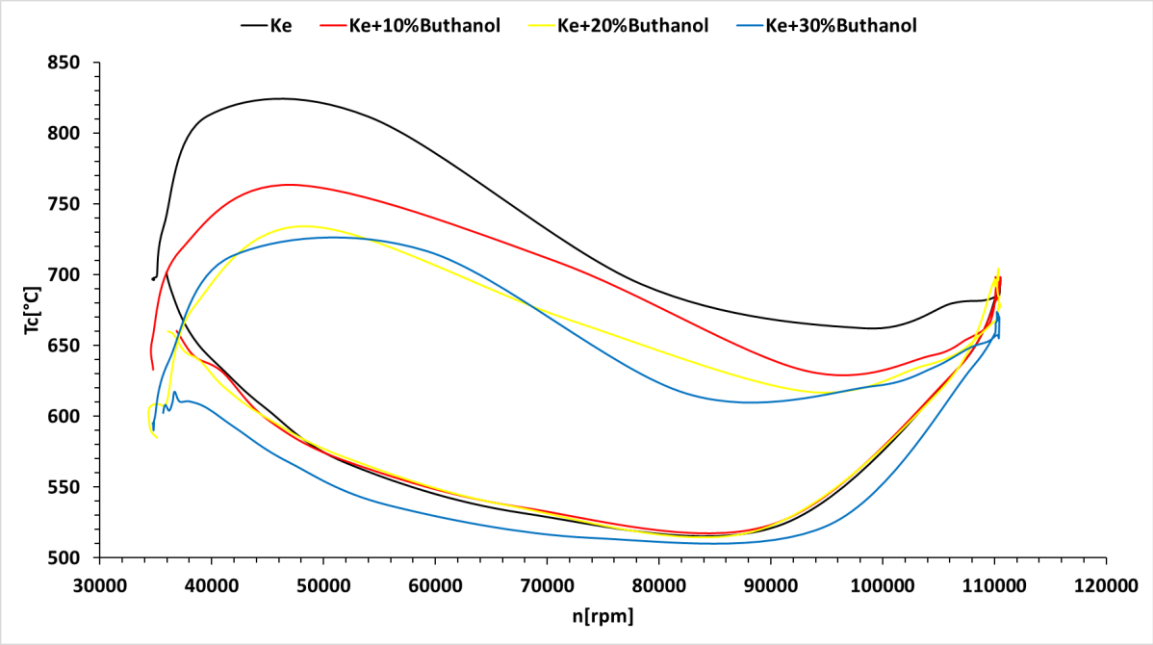


**Figure 7.** The variation of temperature in front of the turbine with respect to RPM during rapid acceleration and deceleration.

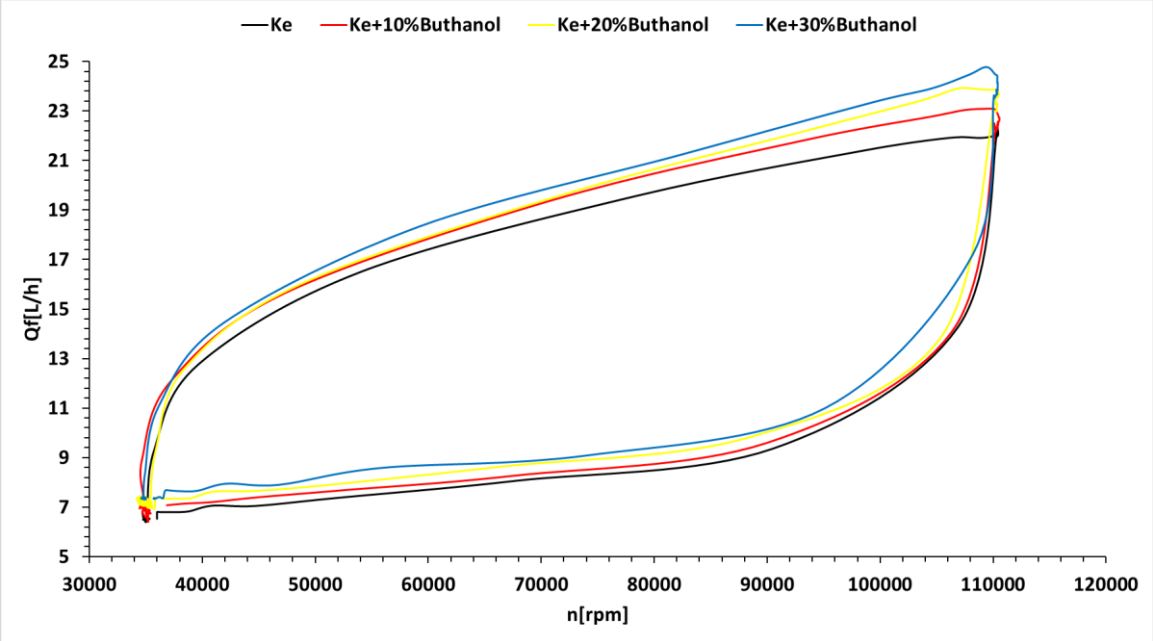

Preprints.org (www.preprints.org) | NOT PEER-REVIEWED | Posted: 10 August 2024 doi:10.20944/preprints202408.0721.v1



**Figure 8.** The variation of fuel flow with respect to RPM during rapid acceleration and deceleration.

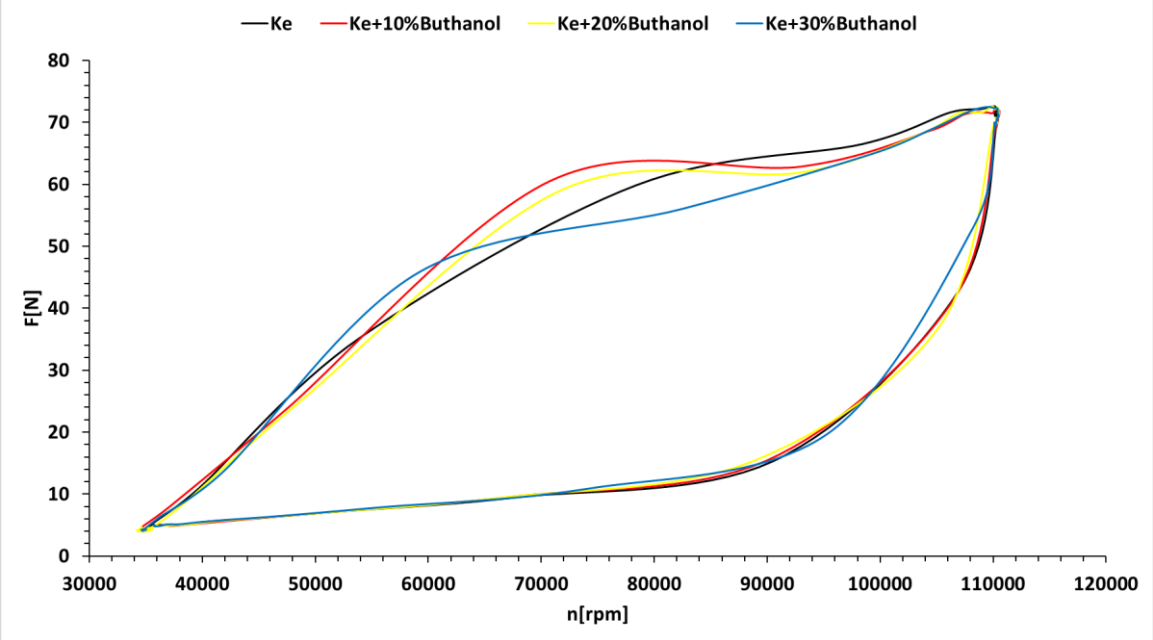


**Figure 9.** The variation of thrust with respect to RPM during rapid acceleration and deceleration.

From the above figures, it can be observed that the micro-turbojet engine underwent rapid acceleration from idle to near maximum, remained at that regime for several seconds, and then decelerated abruptly. During this operation, the combustion temperature decreased as the alcohol concentration increased, although this decrease did not jeopardize the engine's operation and integrity. The fuel flow rate increased as the alcohol concentration increased, as expected due to the lower calorific value of alcohol.

Continuing from the transient regimes, the next stage involved maintaining the engine at three important stable conditions: idle, cruise, and maximum throttle. Figures 10–12 depict the variations in temperature in front of the turbine, fuel flow, and thrust for the analyzed fuels. These parameters were chosen because they are the most critical.

Preprints.org (www.preprints.org) | NOT PEER-REVIEWED | Posted: 10 August 2024 doi:10.20944/preprints202408.0721.v1



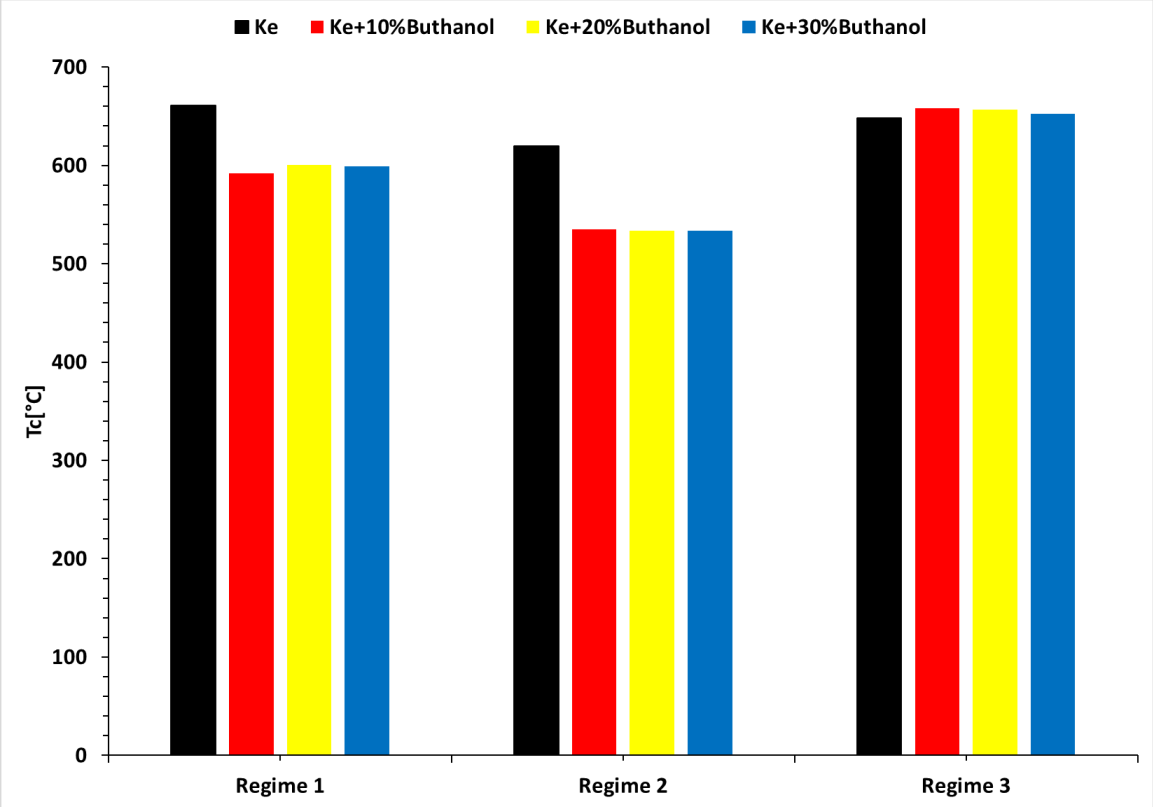


**Figure 10.** Variation of temperature in front of the turbine as a function of regimes and fuel blends.

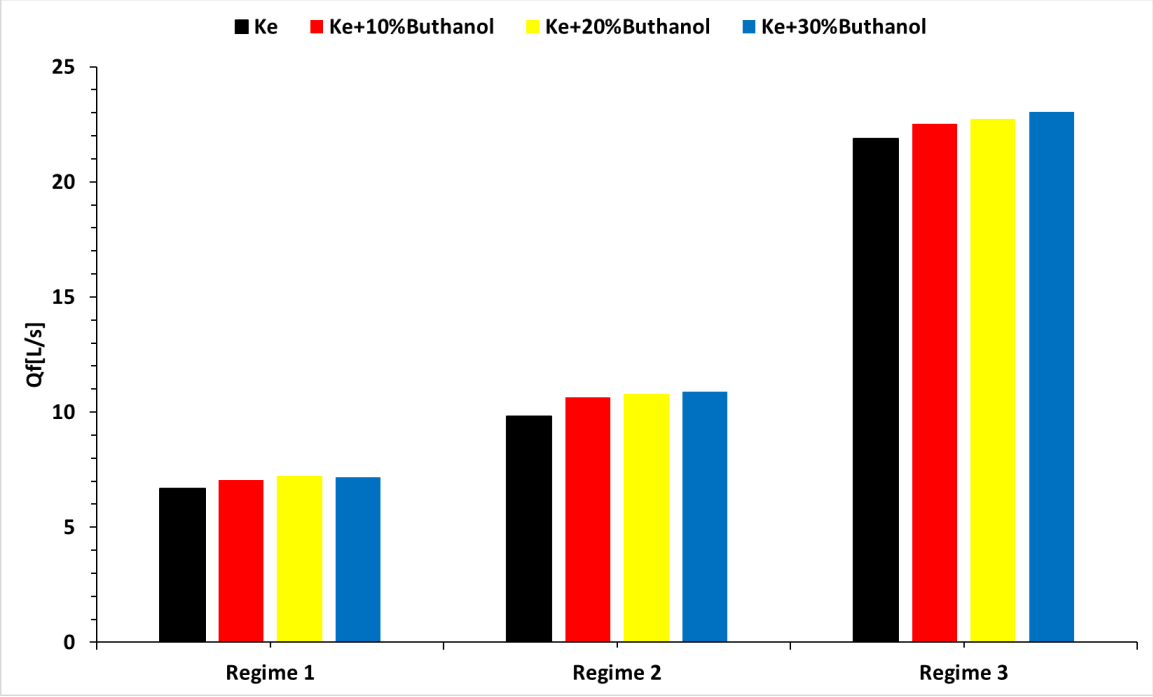


**Figure 11.** Variation of fuel flow as a function of regimes and fuel blends.

Preprints.org (www.preprints.org) | NOT PEER-REVIEWED | Posted: 10 August 2024 doi:10.20944/preprints202408.0721.v1



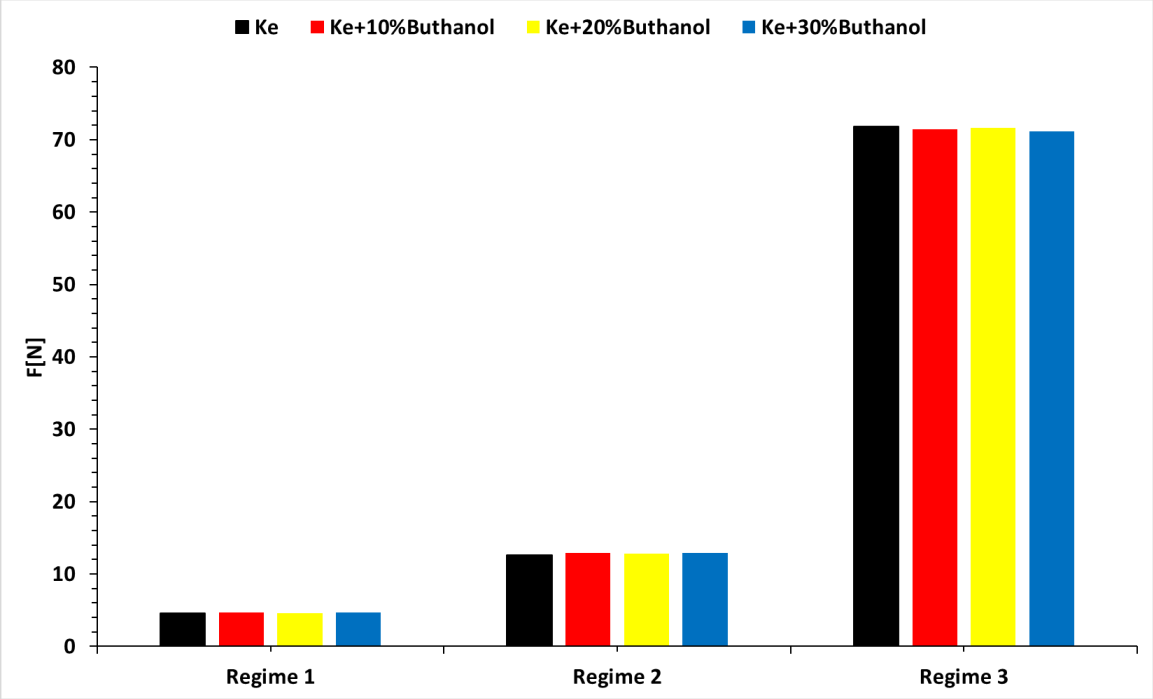


**Figure 12.** Variation of thrust as a function of regimes and fuel blends.

Figure 10 provides a graphical representation of temperature variations in front of the turbine for all three operating regimes and tested fuels.

The analysis indicates that the engine integrity was maintained, as the maximum turbine working temperature of 800°C was neither reached nor exceeded. In idle and cruise regimes, the temperature at the turbine inlet for butanol blends is lower compared to the Jet A reference, while at maximum regime, the turbine inlet temperature shows slightly higher values for butanol blends.

Figure 11 presents the fuel flow rate in liters per hour, revealing a significant increase across all three regimes and tested fuel blends. This observation suggests a notable impact on fuel consumption under different operating conditions, including specific consumption.

Figure 12 illustrates the variations in thrust (F) according to the operating regime and tested fuel blends. In regimes 1 and 2, thrust variations are negligible, but a decrease is observed in regime 3. Additionally, thrust decreases with increasing alcohol concentration. Overall, the analysis of these figures leads to the conclusion that the functionality and integrity of the engine remained intact and unaffected throughout the testing, highlighting the engine's robustness under various operating conditions and fuel blends.

Since the microturbine engine is able to recording of air flow rate and compressor compression ratio, the operating line of the microturbine engine for the four studied fuels was plotted in Figure 13, while Figure 14 illustrates the variation of the microengine's operating line during rapid acceleration and deceleration (variation of compressor pressure range $\pi c$("which can reach a maximum value of around 2.2") vs. air flow $\dot{M}a$, where $\dot{M}a$ is expressed in [kg/s].).

Preprints.org (www.preprints.org) | NOT PEER-REVIEWED | Posted: 10 August 2024 doi:10.20944/preprints202408.0721.v1



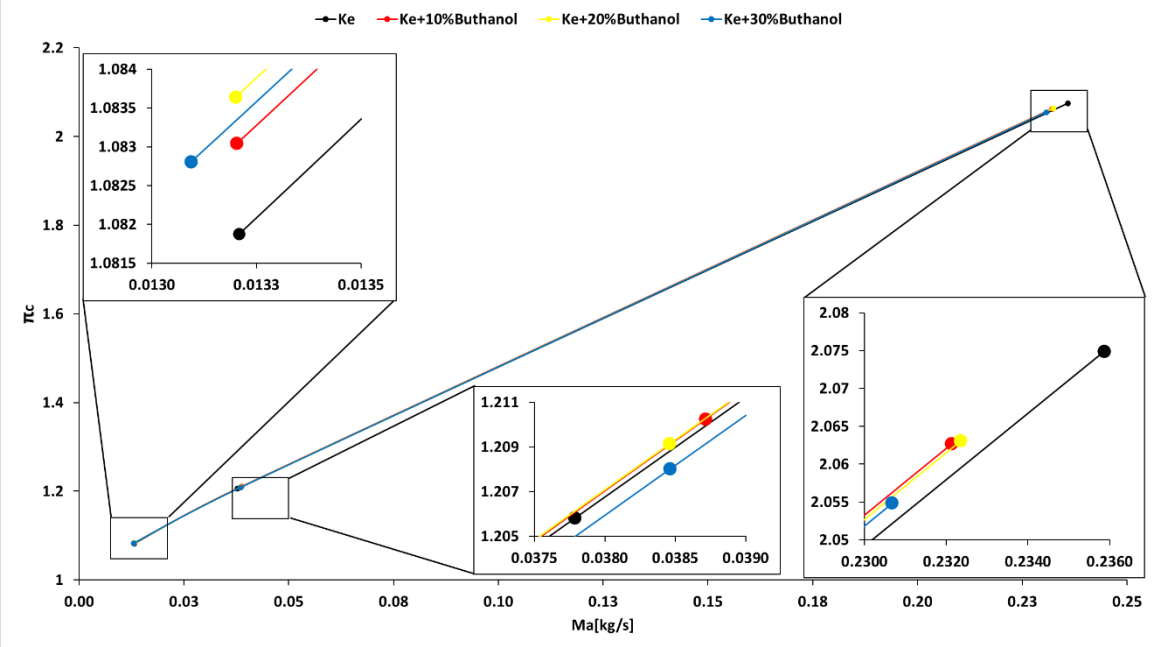


**Figure 13.** Microturboengine operating line.

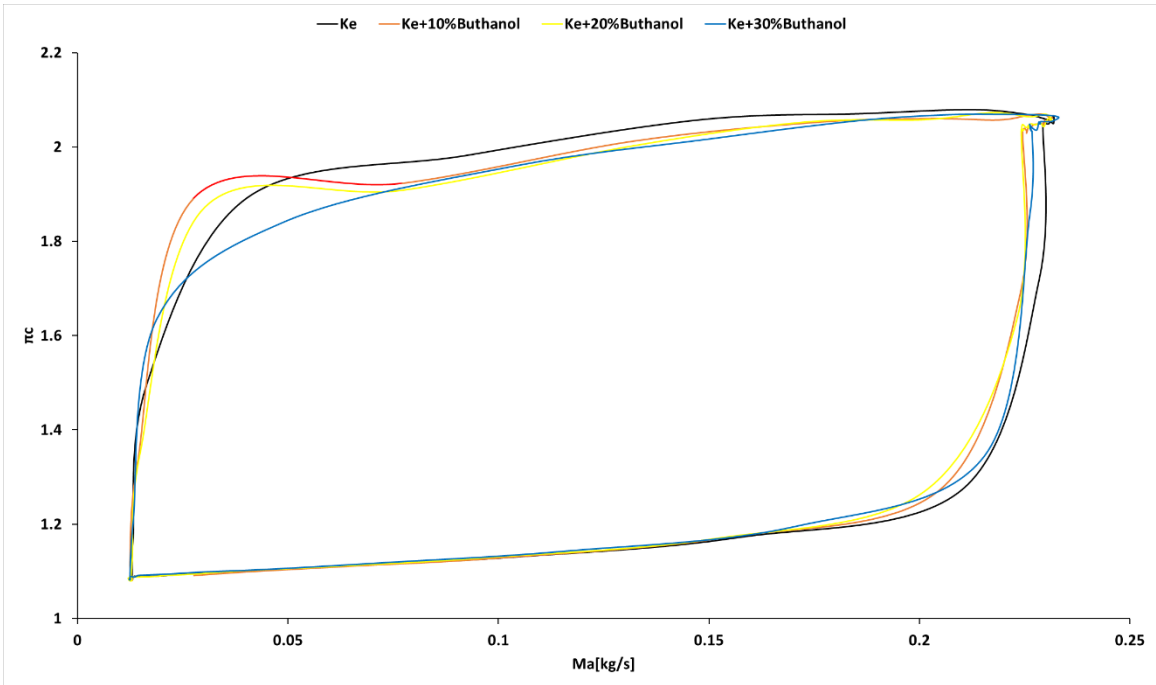


**Figure 14.** Variation of the Microturboengine Operating Line during Rapid Acceleration and Deceleration.

Analyzing Figure 13, it can be observed that the working line shifts when using butanol blends compared to the base fuel, kerosene. This shift is not significant and does not endanger the operation of the micro-turbo engine. Examining Figure 14, it is evident that the working line during rapid acceleration and deceleration deviates considerably from the working line established based on quasi-stationary regimes for all tested fuels, but without causing surge.

For an environmental impact analysis of butanol, the concentration of CO and $SO_2$ was recorded as Figures 15 and 16 illustrate the variations in CO and SO2 levels across all blends and under all three regimes.

Preprints.org (www.preprints.org) | NOT PEER-REVIEWED | Posted: 10 August 2024 doi:10.20944/preprints202408.0721.v1



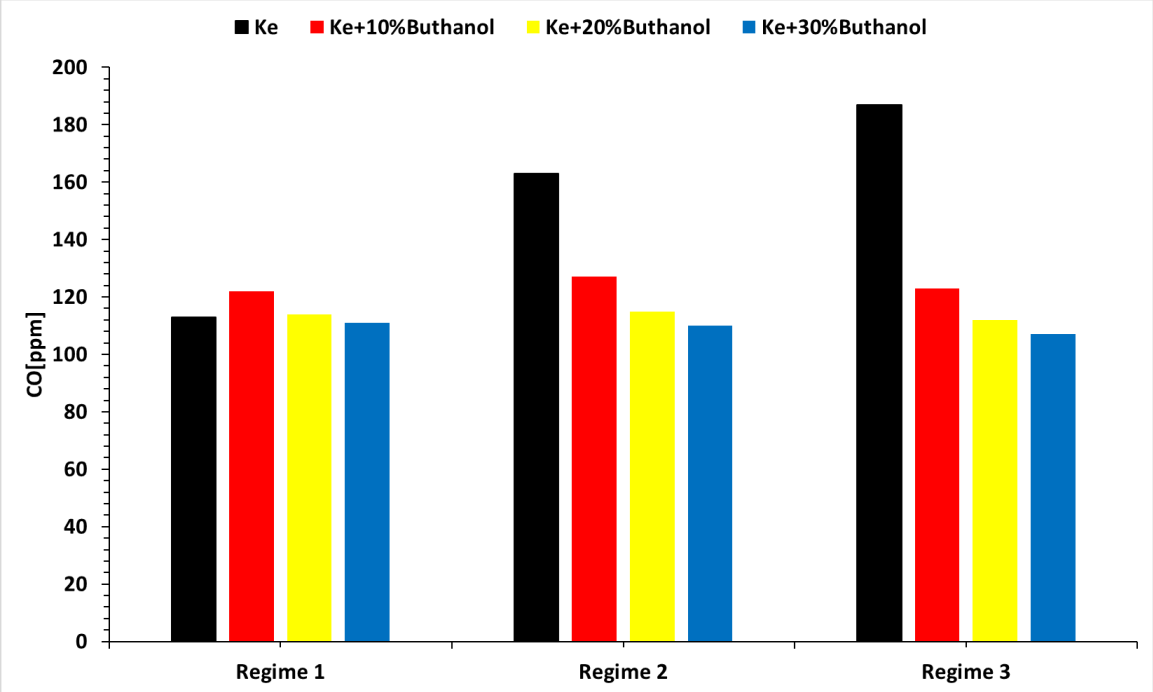


**Figure 15.** The variation in CO concentration for the three regimes and the four fuels analyzed.

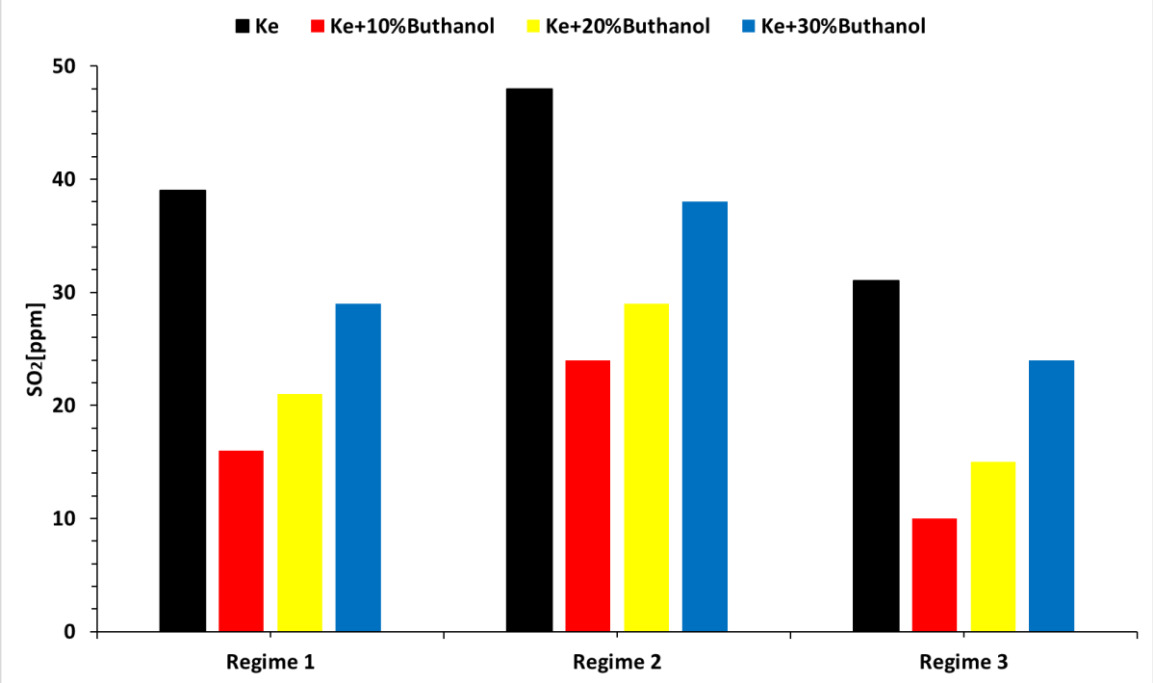


**Figure 16.** The variation in $SO_2$ concentration for the three regimes and the four fuels analyzed.$SO_2$ concentration vs. regimes and blends.

As observed in Figure 15, the CO concentration increases with higher alcohol concentration. This is because alcohol introduces more oxygen into the blend, actively participating in the combustion reaction. Additionally, as the concentration increases, the amount of air needed for the stoichiometric reaction decreases, leading to less efficient combustion and increased CO formation. Temperature strongly influences CO formation, with lower fuel temperatures resulting in higher CO rather than $CO_2$ production. As expected, CO concentration rises across the regimes as fuel flow increases.

Regarding SO2 formation, its variation is independent of alcohol concentration. In fact, compared to pure Ke, adding alcohol increases $SO_2$ concentration due to the additional oxygen

Preprints.org (www.preprints.org) | NOT PEER-REVIEWED | Posted: 10 August 2024 doi:10.20944/preprints202408.0721.v1



introduced by alcohol. In terms of regimes, it appears that for pure Ke, the maximum regime is most efficient in terms of $SO_2$ production because of the higher burning temperatures. However, for blends with added alcohol, the idle regime seems most efficient, likely due to the oxygen introduced by the alcohol reaction.

*3.4. MicroturboJet engine performance analysis*

The performance calculation of the microturbo engine is based on reference [33]. Equation 1 is used to determine the specific consumption. Since the microturbo engine's instrumentation records the fuel flow in L/s, it needs to be converted to kg/s, which requires the density that has been measured.

$$S = 3600 \cdot \frac{\dot{M}f}{F}\left[\frac{kg}{N \cdot h}\right] \quad (5)$$

Where: Mf is the fuel flow in kg/s and F is the thrust.

The next important step is determining the combustion efficiency (ηb) based on experimental measurements. Equation 6 is used to determine combustion efficiency, providing a quantitative measure of the combustion process.

$$\eta_b = \frac{(\dot{M}f + \dot{M}a)cp_{\_comb} \cdot T_{\_comb} - \dot{M}a \cdot cp_{\_comp} \cdot T_{\_comp}}{\dot{M}f \cdot LCP} \quad (6)$$

where: LCP—Lower Calorific Power, cp—specific heat capacity, $T_{comb}$—temperature in front of the combustion chamber (that was recorded), $\dot{M}a$ – the air flow, $T_{comp}$ – temperature after the compressor.

The thermal efficiency of an enginethis parameter, denoted by equation (7), provides a quantitative measure and indicates the capability of converting thermal energy into mechanical work.

$$\eta_T = \frac{(\dot{M}a + \dot{M}f) \cdot v_e^2}{2 \cdot \dot{M}f \cdot LCP} = \frac{(\dot{M}a + \dot{M}f) \cdot \left(\frac{F}{\dot{M}a + \dot{M}f}\right)^2}{2 \cdot \dot{M}f \cdot LCP} \quad (7)$$

Variation of specific consumption for all the tested fuel blends is presented in Figure 17.

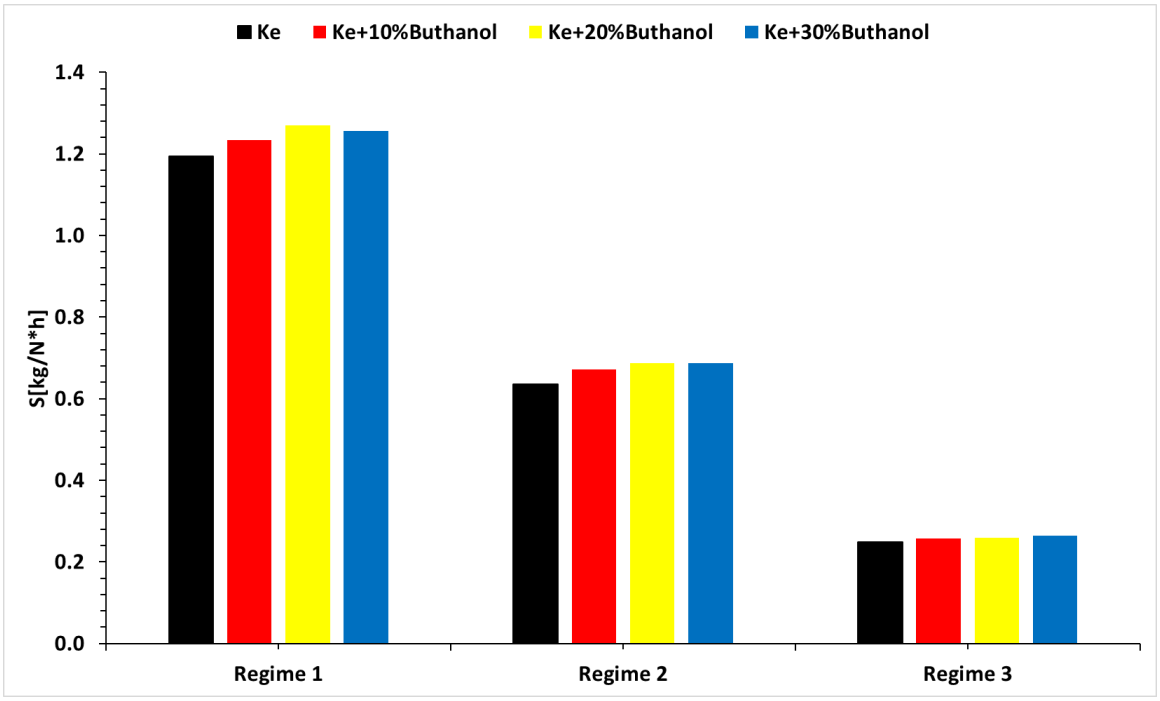


**Figure 17.** The variation of the specific consumption S for the three regimes and the four fuels analyzed.

Preprints.org (www.preprints.org) | NOT PEER-REVIEWED | Posted: 10 August 2024 doi:10.20944/preprints202408.0721.v1



As observed, specific consumption increases with higher alcohol concentration, as expected due to n-butanol's lower calorific value compared to Jet A. Incorporating n-butanol into aviation fuel would require larger tank capacities to offset the increased consumption. This reflects in aircraft design and considerations for storing new fuels.

Figure 18 illustrates combustion efficiency across the three studied regimes and n-butanol concentrations.

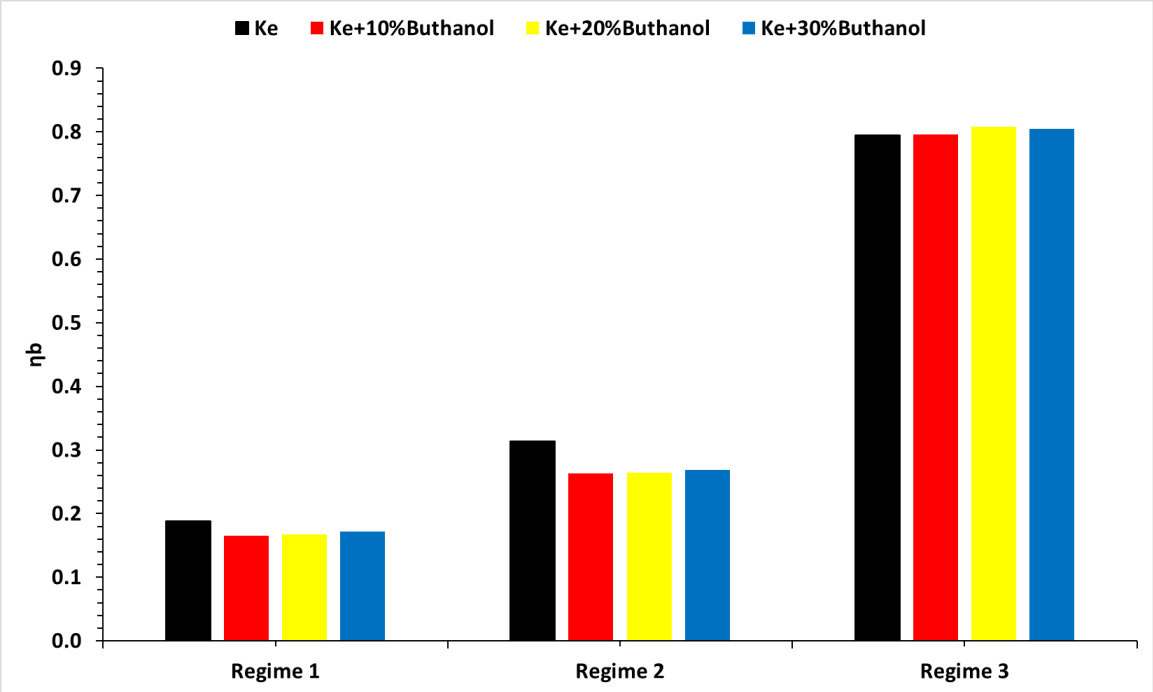


**Figure 18.** The variation of the combustion efficiency for the three regimes and the four fuels analyzed.

Based on Figure 18, it can be observed that combustion efficiency decreases when using Jet A and n-butanol blends for all three studied regimes. Only in regime 3 is combustion efficiency approximately equal across all tested fuel samples. Thermal efficiency of the microturbine engine is presented in Table 3 based on Equation 7.

**Table 3.** Thermal efficiency at the maximum regime for all tested blends.

| Fuel | Ke + 5% Aeroshell 500 Oil | Ke + 10% B | Ke + 20% B | Ke + 30% B |
|---|---|---|---|---|
| $\eta_T$[%] | 5.084 | 5.149 | 5.321 | 5.423 |

The first observation from Table 3 is that thermal efficiency is significantly lower for microturbines compared to large aviation turboengines. It can also be noted that thermal efficiency is slightly higher when increasing the concentration of n-butanol in the tested samples. This highlights the influence of fuel composition on the thermal efficiency of the microturbine engine, emphasizing the need for specific considerations and adjustments in evaluating efficiency in microturbo engine configurations.

## 4. Conclusions

- The experimental evaluations conducted on the Jet CAT P80® micro-turbo engine demonstrate that the inclusion of n-butanol in conventional fuel does not compromise the functionality of the turbo engines.
- The calorific power of the fuel blends experiences a decrease with increasing n-butanol concentration, resulting in a corresponding rise in specific fuel consumption. The lower

Preprints.org (www.preprints.org) | NOT PEER-REVIEWED | Posted: 10 August 2024 doi:10.20944/preprints202408.0721.v1



percentage of carbon in n-butanol, used for blending with Ke (kerosene), contributes to reduced CO2 emissions upon combustion.

- Regarding engine performance, there is a proportional increase in specific fuel consumption with higher n-butanol percentages in the tested blends, a trend attributed to their respective calorific powers.
- As for transient regimes, the micro-turbo engine performed well, with deviations from the kerosene-only case being insignificant both in the starting procedure and in the sudden acceleration and deceleration procedures. The operating line of the micro-turbo engine shows no significant deviations when using kerosene and butanol blends, indicating acceptable stability in transient regimes.
- The concentrations of CO and $SO_2$ vary primarily with operational regimes and secondarily with alcohol concentrations.
- The main conclusion is that the tested fuel blends, namely Ke+10%B, Ke+20%B, and Ke+30%B, are considered suitable for aviation applications using micro-turbo engines. Throughout the experiments, the integrity of the engine remained intact, confirming their viability for practical use in aviation.
- Following experiments on the Jet Cat P80 microturbine engine, it was found that its integrity and functionality were not compromised.
- It can be observed that the calorific power of Jet A and n-butanol blends decreases as the alcohol concentration in the blends increases.
- The amount of $CO_2$ produced during combustion decreases with increasing n-butanol concentration, attributable to the lower carbon content in n-butanol compared to Jet A.
- There is an increase in the specific fuel consumption of the microturbine engine attributed to the calorific power of alcohol.
- The concentration of CO and SO2 is lower when using n-butanol blends.
- As for transient regimes, the micro-turbo engine performed well, with deviations from the kerosene-only case being insignificant both in the starting procedure and in the sudden acceleration and deceleration procedures. The operating line of the micro-turbo engine shows no significant deviations when using kerosene and butanol blends, indicating acceptable stability in transient regimes.
- The primary finding is that the evaluated fuel mixtures—specifically Ke+10%B, Ke+20%B, and Ke+30%B—are deemed appropriate for aviation applications employing micro-turbo engines.

**Author Contributions:** Conceptualization G.C. and R.M.; methodology, G.C. and R.M.; validation, R.M. and G.C.; investigation, R.M.; data curation, R.M. and G.C.; writing—original draft preparation, R.M. and G.C.; writing—review and editing, R.M. and G.C.;. All authors have read and agreed to the published version of the manuscript.

**Conflicts of Interest:** The authors declare no conflict of interest.

**Acknowledgements:** The author would like to acknowledge the financial support the management of INCDT COMOTI.

## References

1. Rhiannon Cordiner, Kai Wan, Shakoor Hajat, Helen L Macintyre, Accounting for adaptation when projecting climate change impacts on health: A review of temperature-related health impacts, Environment International, Volume 188, 2024, 108761, https://doi.org/10.1016/j.envint.2024.108761
2. Wei, H.; Liu, W.; Chen, X.; Yang, Q.; Li, J.; Chen, H. Renewable bio-jet fuel production for aviation: A review. Fuel 2019, 254. [CrossRef]
3. Y.Ye, W. Guo, H. H. Ngo, W. Wei, D. Cheng, X. T. Bui, N. B. Hoang, H. Zhang,
4. F. de O. Gonçalves, E. S. Lopes, M. Savioli Lopes, R. M. Filho, Thorough evaluation of the available light-duty engine technologies to reduce greenhouse gases emissions in Brazil, Journal of Cleaner Production, Volume 358, 2022, 132051, https://doi.org/10.1016/j.jclepro.2022.132051
5. Biofuel production for circular bioeconomy: Present scenario and future scope, Science of The Total Environment, Volume 935, 2024, 172863, https://doi.org/10.1016/j.scitotenv.2024.172863

Preprints.org (www.preprints.org) | NOT PEER-REVIEWED | Posted: 10 August 2024 doi:10.20944/preprints202408.0721.v1




6. Tian, Z.; Zhen, X.;Wang, Y.; Liu, D.; Li, X. Comparative study on combustion and emission characteristics of methanol, ethanol and butanol fuel in TISI engine. Fuel 2020, 259. [CrossRef]
7. S.-R. Jhang, Y.-C. Lin, K.-S. Chen, S.-L. Lin, S. Batterman, Evaluation of fuel consumption, pollutant emissions and well-to-wheel GHGs assessment from a vehicle operation fueled with bioethanol, gasoline and hydrogen, Energy, Volume 209, 2020, 118436, https://doi.org/10.1016/j.energy.2020.118436.
8. Osman, S.; Sapunaru, O.V.; Sterpu, A.E.; Chis, T.V.; I.Koncsag, C. Impact of Adding Bioethanol and Dimethyl Carbonate on Gasoline Properties. Energies 2023, 16, 1940. https://doi.org/10.3390/en16041940
9. Iliev, S. A Comparison of Ethanol, Methanol, and Butanol Blending with Gasoline and Its Effect on Engine Performance and Emissions Using Engine Simulation. Processes 2021, 9, 1322. https://doi.org/10.3390/pr9081322
10. Tibaquirá, J.E.; Huertas, J.I.; Ospina, S.; Quirama, L.F.; Niño, J.E. The effect of using ethanol-gasoline blends on the mechanical, energy and environmental performance of in-use vehicles. Energies **2018**, 11, 221. [CrossRef]
11. Turner, J.; Lewis, A.G.; Akehurst, S.; Brace, C.J.; Verhelst, S.; Vancoillie, J.; Sileghem, L.; Leach, F.; Edwards, P.P. Alcohol fuels for spark-ignition engines: Performance, efficiency and emission effects at mid to high blend rates for binary mixtures and pure components. Automob. Eng. 2018, 232, 36–56. [CrossRef]
12. E. Newes, C. M. Clark, L. Vimmerstedt, S. Peterson, D. Burkholder, D. Korotney, D. Inman, Ethanol production in the United States: The roles of policy, price, and demand, Energy Policy, Volume 161, 2022, 112713,https://doi.org/10.1016/j.enpol.2021.112713.
13. Mirea, R.; Cican, G. Lab Scale Investigation of Gaseous Emissions, Performance and Stability of an Aviation Turbo-Engine While Running on Biodiesel Based Sustainable Aviation Fuel. Inventions 2024, 9, 16. https://doi.org/10.3390/inventions9010016
14. Cican, G.; Crunteanu, D.E.; Mirea, R.; Ceatra, L.C.; Leventiu, C. Biodiesel from Recycled Sunflower and Palm Oil—A Sustainable Fuel for Microturbo-Engines Used in Airside Applications. Sustainability 2023, 15, 2079. https://doi.org/10.3390/su15032079
15. Przysowa, R.; Gawron, B.; Białecki, T.; Ł ¸egowik, A.; Merkisz, J.; Jasi ´nski, R. Performance and Emissions of a Microturbine and Turbofan Powered by Alternative Fuels. Aerospace 2021, 8, 25. https://doi.org/10.3390/ aerospace8020025
16. Labeckas, G.; Slavinskas, S.; Laurinaitis, K. Effect of jet A-1/ethanol fuel blend on HCCI combustion and exhaust emissions. J. Energy Eng. 2018, 144. [CrossRef]
17. Shauck, M.E.; Tubbs, J.; Zanin, M.G. Certification of a Carburater Aircraft Engine on Ethanol Fuel. Available online: https: //afdc.energy.gov/files/pdfs/2896.pdf (accessed on 18 May 2024).
18. Litt, J.S.; Chin, J.C.; Liu, Y. Simulating the Use of Alternative Fuels in a Turbofan Engine; National Aeronautics and Space Administration, Glenn Research Center: Cleveland, OH, USA, 2013.
19. Gawron, B.; Białecki, T.; Dzi¸egielewski,W.; Ka´zmierczak, U. Performance and emission characteristic of miniature turbojet engine FED Jet A-1/alcohol blend. J. KONES 2016, 23. [CrossRef]
20. Mendez, C.J.; Parthasarathy, R.N.; Gollahalli, S.R. Performance and emission characteristics of butanol/Jet A blends in a gas turbine engine. Appl. Energy 2014, 118, 135–140. [CrossRef]
21. Andoga, R.; F˝oz˝o, L.; Schrötter, M.; Szabo, S. The Use of Ethanol as an Alternative Fuel for Small Turbojet Engines. Sustainability 2021, 13, 2541. https://doi.org/ 10.3390/su13052541
22. Cican, G., Deaconu, M., Mirea, R., Cucuruz, A.T., Influence of Bioethanol Blends on Performances of a Micro Turbojet Engine, Rev. Chim., 71(5), 2020, 229-238. https://doi.org/10.37358/RC.20.5.8131
23. Chen, L.; Zhang, Z.; Lu, Y.; Zhang, C.; Zhang, X.; Zhang, C.; Roskilly, A.P. Experimental study of the gaseous and particulate matter emissions from a gas turbine combustor burning butyl butyrate and ethanol blends. Appl. Energy 2017, 195, 693–701. [CrossRef]
24. Cican, G.; Mirea, R.; Rimbu, G. Experimental Evaluation of Methanol/Jet-A Blends as Sustainable Aviation Fuels for Turbo-Engines: Performance and Environmental Impact Analysis. Fire 2024, 7, 155. https://doi.org/10.3390/fire7050155
25. European Committee for Standardization. SR EN ISO 3675/2003, Crude Petroleum and Liquid Petroleum Products—Laboratory Determination of Density—Hydrometer Method; ASRO: Bucharest, Romania, 2003.
26. ASTM International. ASTM D92-05a, Standard Test Method for Flash and Fire Points by Cleveland Open Cup Tester; ASTM International: West Conshohocken, PA, USA, 2009.
27. European Committee for Standardization. SR EN ISO 3104/2002, Petroleum Products. Transparent and Opaque Liquids. Determination of Kinematic Viscosity and Calculation of Dynamic Viscosity; ASRO: Bucharest, Romania, 2002.
28. ASTM International. ASTM D240-17, Standard Test Method for Heat of Combustion of Liquid Hydrocarbon Fuels by Bomb Calorimeter; ASTM International: West Conshohocken, PA, USA, 2017.
29. ASTM D5291-16. Standard Test Methods for Instrumental Determination of Carbon, Hydrogen, and Nitrogen in Petroleum Products and Lubricants; ASTM International: West Conshohocken, PA, USA, 2016.
30. Jet Cat USA. Jet Cat Instruction Manual. U.S. Patent No. 6216440, 17 April 2001.

Preprints.org (www.preprints.org) | NOT PEER-REVIEWED | Posted: 10 August 2024 doi:10.20944/preprints202408.0721.v1



31. Lois, A.L. Biodiesel and Biokerosenes: Production, Characterization, Soot & Pah Emissions. Ph.D. Thesis, Polytechnic University of Madrid, Madrid, Spain, 2015.
Oyerinde, A.Y.; Bello, E.I. Use of Fourier Transformation Infrared (FTIR) Spectroscopy for Analysis of Functional Groups in Peanut Oil Biodiesel and Its Blends. Br. J. Appl. Sci. Technol. 2016, 13, 22178. [CrossRef]
32. J.G. Speight Handbook of Industrial Hydrocarbon Processes, Gulf Professional Publishing, 2020, ISSN 978-0-12-809923-0
33. Mattingly, J. Elements of Propulsion: Gas Turbines and Rockets, 2nd ed.; American Institute of Aeronautics and Astronautics: Reston, VA, USA, 2006.
34. Cican, G. Experimental Transient Process Analysis of Micro-Turbojet Aviation Engines: Comparing the Effects of Diesel and Kerosene Fuels at Different Ambient Temperatures. Energies 2024, 17, 1366. https://doi.org/10.3390/en17061366

**Disclaimer/Publisher's Note:** The statements, opinions and data contained in all publications are solely those of the individual author(s) and contributor(s) and not of MDPI and/or the editor(s). MDPI and/or the editor(s) disclaim responsibility for any injury to people or property resulting from any ideas, methods, instructions or products referred to in the content.